DISCOVERY AND MODELLING OF DISC PRECESSION IN THE M31 X-RAY BINARY BO 158

R. Barnard [1], **S.B. Foulkes**[1], **C.A. Haswell**[1], **U. Kolb**[1], **J.P. Osborne**[2], **and J.R. Murray**[3]

[1]Department of Physics and Astronomy, The Open University, Walton Hall, Milton Keynes, UK MK7 6AA
[2]Physics and Astronomy, The University of Leicester, Leicester, UK, LE1 7RH
[3]Swinburne University of Technology, Australia

ABSTRACT

The low mass X-ray binary (LMXB) associated with the M31 globular cluster Bo 158 is known to exhibit intensity dips on a $\sim$2.78 hr period. This is due to obscuration of the X-ray source on the orbital period by material on the outer edge of the accretion disc. However, the depth of dipping varied from $<$10% to $\sim$83% in three archival XMM-Newton observations of Bo 158. Previous work suggested that the dip depth was anticorrelated with the X-ray luminosity. However, we present results from three new XMM-Newton observations that suggest that the evolution of dipping is instead due to precession of the accretion disc. Such precession is expected in neutron star LMXBs with mass ratios $<$0.3 (i.e. with orbital periods $<$4 hr), such as the Galactic dipping LMXB 4U 1916$-$053. We simulated the accretion disc of Bo 158 using cutting-edge 3D smoothed particle hydrodynamics (SPH), and using the observed parameters. Our results show disc variability on two time-scales. The disc precesses in a prograde direction on a period of 81 ± 3 hr. Also, a radiatively-driven disc warp is present in the inner disc, which undergoes retrograde precesson on a $\sim$31 hr period. From the system geometry, we conclude that the dipping evolution is driven by the disc precession. Hence we predict that the dipping behaviour repeats on a $\sim$81 hr cycle.

Key words: X-rays: general; X-rays: binaries; Galaxies: individual: M31, Accretion: accretion discs.

1. INTRODUCTION

Bo 158 is source number 158 in the catalogue of globular clusters that were identified in M31 by Battistini et al. (1987). Its X-ray counterpart is located at α = $00^{\rm h}43^{\rm m}14.2^{\rm s}$, δ = $41^\circ07'26.3''$ (Di Stefano et al., 2002). Trudolyubov et al. (2002) identified the X-ray source as a likely low mass X-ray binary (LMXB) with a neutron star primary; following their work, we will use the designation "Bo 158" to describe the X-ray source here.

Trudolyubov et al. (2002) report $\sim$83% modulation in the 0.3–10 keV flux of Bo 158 on a 2.78 hour period during the $\sim$60 ks 2002 January XMM-Newton observation. The modulation resembles the intensity dips seen in high inclination LMXBs due to photo-electric absorption of X-rays by material that is raised above the body of the accretion disc (White & Swank, 1982). They also report $\sim$30% dips in the 2000, June XMM-Newton lightcurve and $\sim$50% dips in the 0.2–2.0 keV lightcurve of the 1991, June 26 ROSAT/PSPC observation. However, no significant dips were found in the 0.3–10 keV lightcurve of the 2001 June XMM-Newton observation; the authors placed a 2σ upper limit of 10% on the modulation. Trudolyubov et al. (2002) concluded that the depth of the intensity modulation was anti-correlated with the source luminosity.

We present further XMM-Newton observations and modelling results which suggest that the variation in dipping behaviour may instead be due to precession of the accretion disc. Such behaviour is associated with the "superhump" phenomenon that is observed in interacting binaries where the mass ratio of the secondary to the primary is smaller than $\sim$0.3 (Whitehurst & King, 1991). Superhumps are briefly reviewed in Sect. 2, followed by details of the observations and data analysis in Sect. 3, and our results in Sect. 4. Numerical modelling of the system is discussed in Sect. 5; the system was simulated by a 3D smoothed particle hydrodynamics (SPH) code. We present our discussion in Sect. 6, and finally our conclusion in Sect. 7.

2. SUPERHUMPS

Superhumps were first identified in the superoutbursts of the SU UMa sub-class of cataclysmic variables. They are manifested as a periodic increase in the optical brightness on a period that is a few percent longer than the orbital period (Vogt, 1974; Warner, 1975). In the model proposed by Osaki (1989), superhumps occur when the outer disc reaches a 3:1 resonance with the secondary. The additional tidal forces exerted on the disc by the secondary

Table 1. Journal of XMM-Newton observations of the M31 core. A1–A3 are available in the public archive, while P4–P6 are proprietary observations. Two observations were made during 2004 July 19; the first observation (a) started at 01:42:12, and the second (b) started at 13:11:22.

Observation	Date	Exp	Filter
A1	2000 Jun 25	34 ks	Medium
A2	2001 Jun 29	56 ks	Medium
A3	2002 Jan 6	61 ks	Thin
P4	2004 Jul 17	18 ks	Medium
P5	2004 Jul 19a	22 ks	Medium
P6	2004 Jul 19b	27 ks	Medium

at this stage cause the disc to elongate and precess, and also greatly enhance the loss of angular momentum, increasing the the mass-transfer rate. The disc precession is prograde in the rest frame, and the secondary repeats its motion with respect to the disc on the beat period between the orbital and precession periods, slightly longer than the orbital period. The secondary modulates the disc's viscous dissipation on this period, giving rise to maxima in the optical lightcurve, known as superhumps.

The requirement for the 3:1 resonance to fall within the disc's tidal radius is that the mass ratio of the secondary to the primary be less than $\sim$0.33 (Whitehurst & King, 1991). If we assume that the secondary is a main sequence star that fills its Roche lobe, then the relation $m_2 \simeq 0.11\,P_{\rm hr}$ holds, where m_2 is the mass of the secondary in solar units and $P_{\rm hr}$ is the orbital period in hours (e.g. Frank, King, & Raine, 2002). Hence any accreting binary that has a short enough orbital period may exhibit superhumps.

3. OBSERVATIONS AND DATA ANALYSIS

In addition to the three XMM-Newton observations analysed by Trudolyubov et al. (2002), we conducted a programme of four $\sim$20 ks observations over 2004, July 16–19. We present results from our analysis of the archival data, along with three of the four 2004 observations; the other observation suffered from flaring in the particle background over 90% of the observation and is not considered further here. A journal of observations is presented in Table 1.

We analysed data from the pn, MOS1 and MOS2 instruments, which share the same $30'' \times 30''$ field of view. For each observation, we selected a circular extraction region with a $40''$ radius, centred on Bo 158, and an equivalent source-free region for the background. The background region was on the same chip as the source, and at a similar angular offset from the optical axis. We extracted lightcurves from the source and background regions in the 0.3–10 keV energy band with 2.6 s binning, and also obtained pn spectra of the source and background regions along with the associated response files. The spectra were then grouped for a minimum of 50 counts per bin.

4. RESULTS

The 0.3–10 keV EPIC (MOS1 + MOS2 + pn) lightcurves of Observations A1–A3 are presented in Fig. 1, with x- and y- axes set to the same scale, and with 200 s binning. Most striking is Observation A3, with six dipping intervals on a 10017 ± 50 second period (Trudolyubov et al., 2002); the structure of the dipping is seen to vary substantially even over one observation of 60 ks. We emphasise that the 30% dipping reported by Trudolyubov et al. (2002) for observation A1 is an overall average; a deep dip is seen at $\sim$28 ks into the observation, but very little evidence of dipping is observed in the intervals of expected dipping at $\sim$8 ks and $\sim$18 ks into the observation. In this regard, Observation A1 resembles the 1985, October lightcurve of the Galactic superhumping LMXB 4U 1916$-$053, observed by EXOSAT. In that observation, deep dips are observed only after the first four orbital cycles (Smale et al., 1988). Little evidence of variability is seen in the lightcurve of Observation A2.

In Fig. 2, we present the 0.3–10 keV EPIC lightcurves of Observations P4–P6; the x-axis is scaled to P6, and the y-axis matches that of Fig. 1. The most prominent feature is the dip in P5; it has a depth of $\sim$100% and a total duration of $\sim$2500 s. Using the period of Trudolyubov et al. (2002), we identified the expected times of dipping, labelled 'D', in P4 and P6, using the deepest part of the dip in P5 as phase zero.

In the P4 lightcurve, there is no evidence for dipping during the first expected dip interval, but some evidence of dipping $\sim$4000 s after the second interval, 20 cycles away from the dip in P5. Hence, this possible dip would require a period that is either $\sim$200 s shorter or $\sim$320 s longer than the 10017 s given by Trudolyubov et al. (2002). However, there is no other evidence for these other periods in the lightcurves of P4, P5 or P6; hence it is clear that the dipping behaviour of Bo 158 evolves on a time scale of a few days.

Several spectral models were fitted to the 0.3–10 keV pn spectrum of P4, each suffering absorption by material in the line of sight. P4 was chosen because it had the longest interval of persistent emission that was not contaminated by background flares; the resulting source spectrum contained $\sim$2200 counts. We applied the two models that Trudolyubov et al. (2002) used to model the spectra of A1–A3, namely a power law model and a Comptonisation model (COMPTT in XSPEC). We also applied a two component model. The emission of many Galactic LMXBs has been succesfully described by a model consisting of a blackbody and a cut-off power law (e.g. Church & Bałucińska-Church, 1995; Church et al., 1998; Barnard et al., 2003); we approximate this model to a blackbody + power law model, because of the narrow pass-band.

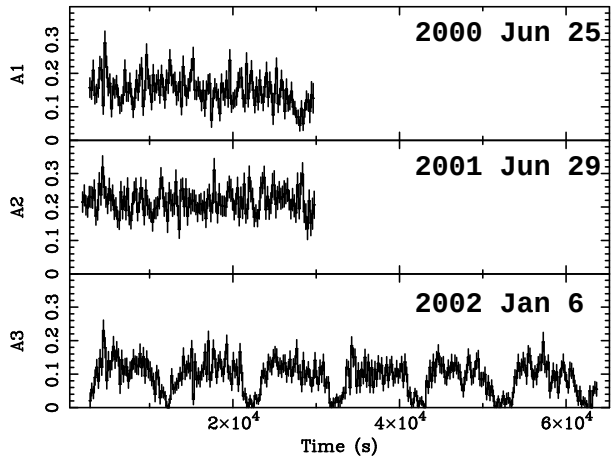

Figure 1. Combined EPIC 0.3–10 keV lightcurves (in count s^{-1}) of Bo 158 from the archival XMM-Newton observations, A1–A3; the dates of each observation are shown.

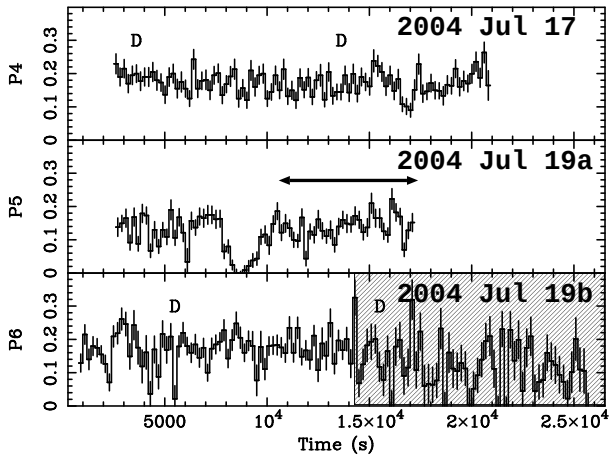

Figure 2. Combined EPIC 0.3–10 keV lightcurves (in count s^{-1}) of Bo 158 from the 2004 XMM-Newton observations, P4–P6; the dates of each observation are shown. The horizontal line in the P5 lightcurve indicated the interval used for spectral fitting. The shaded area of the P6 lightcurve indicates a period of background flaring. Times when dipping is expected are labelled "D", using the deepest part of the dip in P5 as time zero, and the period of Trudolyubov et al. (2002).

We find that the best fit parameters for the power law and COMPTT models agree well with the values presented by Trudolyubov et al. (2002); however, the two-component model provided the best fit. We find a 0.3–10 keV flux of $\sim 2\times10^{-12}$ erg cm^{-2} s^{-1} for all the fits to the P4 data; this gives a 0.3–10 keV luminosity of $\sim 1.4\times10^{38}$ erg s^{-1}, assuming a distance of 760 kpc (van den Bergh, 2000).

The depth of dipping in A1 varies from $\sim$0 to $\sim$70% with no significant change in the mean intensity, suggesting that the amplitude of dipping is not simply anticorrelated with the source luminosity. Instead, the variation in dipping behaviour may be caused by disc precession. This hypothesis motivated our simulation of the accretion disc in Bo 158, using three dimensional smoothed partical hydrodynamics, discussed in Sect. 5.

The lightcurves of XMM-Newton observations of Bo 158 show no true eclipses; hence, we know that we are not viewing the system edge on. If the disc were tilted with respect to the binary plane, and precessing, then one might expect to observe dips in some part of the disc precession cycle, but not in others. Dipping is observed throughout observation A3; this suggests that the dipping phase in the disc precession cycle lasts $> \sim$60 ks. The A1 lightcurve covered three intervals of expected dipping, yet only one dip is seen, toward the end of the observation; we suggest that this dip signals the onset of the dipping phase. Contrariwise, P5 and P6 appear to sample the end of the dipping phase, as a dip is observed in P5, yet no dips are seen in P6.

5. SPH SIMULATION OF THE DISC

5.1. Binary Parameters

The accretion disc was modelled using a three-dimensional Smoothed Particle Hydrodynamics (SPH) computer code that has been described in detail in Murray (1996, 1998), Truss et al. (2000), and Foulkes, Haswell, & Murray (2006). We assumed the orbital period to be 10017 s, as obtained by Trudolyubov et al. (2002).

The dipping source Bo 158 is a bright globular cluster X-ray source, with a 2.78 hr binary period. Thirteen Galactic globular clusters contain bright X-ray sources; twelve of these are neutron star LMXBs, while the primary of the other one is unknown (see e.g. in't Zand et al., 2004). Hence Bo 158 is a likely neutron star LMXB, and we assume the primary mass to be 1.4 $M_\odot$.

For the secondary, we considered a main sequence star and a white dwarf, since 4U 1916$-$053 has a likely white dwarf secondary (e.g. Chou et al., 2001). For a Roche lobe-filling main sequence star the approximate relation m $\simeq$ 0.11 $P_{\rm hr}$ holds (e.g. Frank et al., 2002), giving a mass of $\sim$0.30 $M_\odot$. If instead the star is a white dwarf, using the mass radius relation of Nauenberg (1972) and Roche geometry gives an implausibly small mass of 0.005 $M_\odot$. Assuming a main sequence secondary, we found the mass ratio to be 0.2, indicating that superhumps and disc precession were likely.

Finally, the luminosity of the system was taken to be 1.4×10^{38} erg s^{-1}, the 0.3–10 keV luminosity of Bo 158

in Observation P4. Such a high luminosity may be expected to cause warping of the accretion disc, even for a previously flat disc (see e.g. Pringle, 1996); warping is discussed in Sect. 5.3.

The accretion disc had an open inner boundary condition in the form of a hole of radius $r_1 = 0.025a$, where a is the binary separation, centred on the position of the primary object. Particles entering the hole were removed from the simulation. Particles that re-entered the secondary Roche lobe were also removed from the simulation as were particles that were ejected from the disc at a distance $> 0.9a$ from the centre of mass.

We assumed an isothermal equation of state and that the dissipated energy was radiated from the point at which it was generated, as electromagnetic radiation. The Shakura & Sunyaev (1973) viscosity parameters were set to α_{low} = 0.1 and α_{high} = 1.0, and the viscosity state changed smoothly as described in Truss et al. (2000). The SPH smoothing length, h, was allowed to vary in both space and time and had a maximum value of $0.01a$.

5.1.1. The gas stream

We simulated the mass loss from the secondary by introducing particles at the inner Lagrangian point (L_1). The mass transfer rate and the particle transfer rate were provided as input parameters, and the mass of each particle was derived from these parameters. A particle was inserted with an initial velocity (in the orbital plane) equal to the local sound speed of the donor, $c_{\rm D}$, in a direction prograde of the binary axis. The z velocity of the inserted particle was chosen from a Gaussian distribution, with a zero mean and a variance of $0.1c_{\rm D}$. However, the inflation of the site of collision between the gas stream and outer disc was not modelled.

5.1.2. The initial non-warped accretion disc

The simulation was started with zero mass in the accretion disc and with the central radiation source switched off. A single particle was injected into the simulation every $0.01\Omega_{orb}^{-1}$ at the L_1 point as described above until a quasi-steady mass equilibrium was reached within the disc. This was taken to be when the number of particles inserted at the L_1 point, the mass transfer rate, was approximately equal to number of particles leaving the simulation at the accretor, the accretion rate. The simulations were continued for another 3 orbital periods to ensure mass equilibrium. The number of particles in the simulated accretion disc was approximately 40,000 giving a good spatial resolution; the average number of 'neighbours', i.e. the average number of particles used in the SPH update equations, was 8.2 particles. The simulated disc encountered the Lindblad 3:1 resonance and became eccentric. The disc precessed in a prograde direction giving rise to superhumps in the simulated dissipation lightcurves (c.f. Foulkes et al., 2004). The radiation source was then turned on which gave rise to a very small number of particles being ejected from the accretion disc.

5.2. Surface finding algorithm & self-shadowing

Accretion-powered radiation from the inner regions of the disc and the accreting object itself exert a force on the irradiated disc surface. Following Pringle (1996) the radiation source is modelled as a point source at the centre of mass of the accretor. To apply this force, particles on the surface of the accretion disc had to be identified. We used a convex hull algorithm to find the surface particles as described in Murray (1998) and Foulkes et al. (2006). A ray-tracing algorithm was used to determine regions of self-shadow. For each particle found on the disc surface a light-ray was projected from the particle to the position of the radiation source at the centre of the disc. The particle was deemed to be illuminated by the radiation source if this light-ray did not intersect any disc material between the particle surface position and the radiation source (i.e. the particle could see the central radiation source). The radiation force was only applied to particles that were considered to form part of the disc surface and were illuminated by the central radiation source.

5.3. Disc warping and precession measure

For an optically thick disc, a warp can develop as a result of the radiation force (e.g. Pringle, 1996; Ogilvie & Dubus, 2001; Foulkes et al., 2006). This is due to the fact that any radiation absorbed by a specific region on the disc surface will be later re-radiated from the same spot, normal to the disc surface. Hence any anisotropy in the disc structure will cause an uneven distribution of back-reaction forces on the disc surface, further perturbing the disc. A sufficiently high luminosity can induce and sustain a warp even in an originally flat disc (Pringle, 1996, and references therein).

5.4. Numerical modelling results

As a result of the disc precession, viscous stresses in the disc vary significantly with time. The resultant energy dissipation in different regions of the disc, and hence the disc luminosity, varies with time. The disc luminosity was not modelled in detail. We assumed that the luminosity was directly related to the disc regions with significant energy release through viscous dissipation. The viscous dissipation heats the gas in the accretion disc and it is assumed that the heat is radiated away from the point at which it was generated. Superposed on a steady signal there is a repeating series of "humps." The spacing of the humps corresponds to the superhump period, but are not representative of true optical lightcurves.

In order to determine the superhump period, $P_{\rm sh}$, we obtained a power density spectrum from $\sim$30 superhump

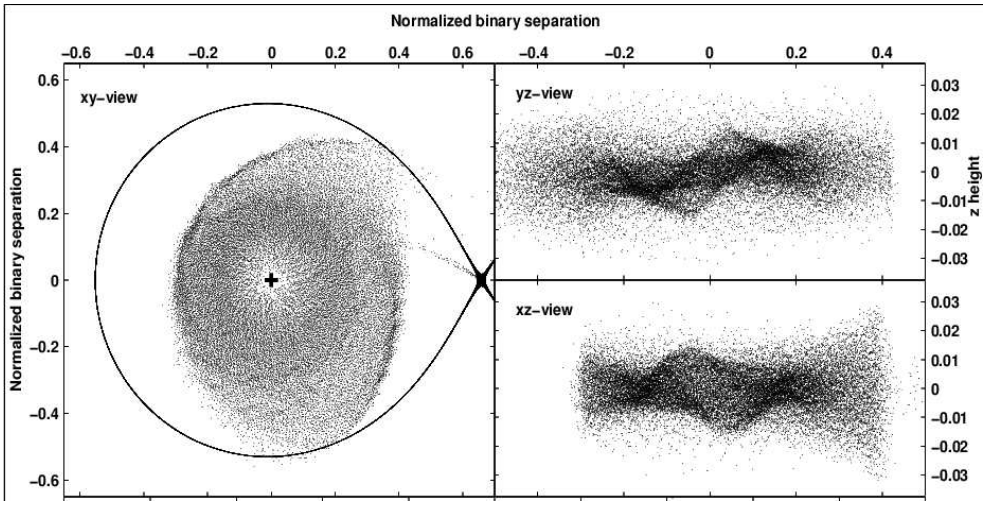

Figure 3. Particle projection plots for the SPH model. The position of each particle is indicated by a small black dot. The left panel is a plan view of the accretion disc as seen from above the disc. The cross at the centre of the plot shows the position of the primary object. The solid dark line is the Roche lobe of the primary and the L_1 point is to the right and middle of the plot. The right panels are are particle projection plots on a plane perpendicular to the orbital plane and through the system axis in the xz and yz directions.

cycles of the simulated light curve. We estimated the superhump period to be $(1.035 \pm 0.005)P_{\rm orb}$. This implies the precession period of the outer regions, $P_{\rm prec} = (29 \pm 1)P_{\rm orb}$, or 81±3 hr.

Fig. 3 shows a snapshot from the simulation, from several different angles. The left panel shows an x-y projection of the disc. The disc is clearly asymmetric and elongated, and a spiral density wave is clearly seen. This wave is so intense that it is removing material from the accretion disc and returning it back to the Roche lobe of the secondary; see Foulkes et al. (2004) for a full detailed description of a similar system with a mass ratio of 0.1.

The two upper right-hand plots of Fig. 3, labelled yz-view and xz-view, are side views of the disc in the y-z and x-z directions respectively. The disc warp is clearly apparent in these two plots. The warp is odd symmetrical about the centre of the disc.

The warp amplitude and size precessed as a solid body in a retrograde direction relative to the inertial frame. We found that $P_{\rm warp} \sim 11\,{\rm P_{orb}}$. Fig. 4 shows the radial profile of the warp for five consecutive orbital cycles; the maximum extent of the warp is 6–11° above the plane of the disc.

6. DISCUSSION

Disc precession is inferred from the 0.3–10 keV lightcurves of Bo 158, as is expected given its extreme mass ratio (short orbital period). As such, it resembles the Galactic superhumping LMXB 4U 1916−053. Since the LMXB Bo 158 is in a globular cluster near the centre of M31, it is unlikely that the optical period will ever be known. However, our Fourier analysis of the simulated dissipation lightcurves indicates a superhump period that is 3.5±0.5% longer than the orbital period. Given the association between the dips and superhump period reported by Retter et al. (2002), the 10017 s period may be the superhump period, in which case, the orbital period would be ∼4% shorter. Such shortening of the period would not dramatically affect the outcome of our SPH modelling.

Our simulations of the disc show two distinct types of variability in the disc structure. First is the elongation and prograde precession of the disc due to tidal interactions with the secondary at the 3:1 resonance; the disc precesses on period of 81±3 hr. We also see warping of the accretion disc, driven by irradiation of the disc surface by the central X-ray source; the warp is stable exhibits retrograde precession on a ∼31-hr period.

It is therefore important to establish which region is responsible for the observed variation in dip morphology. The lightcurves of observations A1–P6 show no eclipses. From Kepler's law and the ratio of the secondary ratio to the binary separation (Eggleton, 1983), the secondary has an angular radius of ∼15°; hence the inclination > ∼75°. We see from Fig. 6 that the disc warp does not deviate from the plane of the disc by more than 11° in our simulations, suggesting that the observed dips are likely to evolve on the disc precession period.

7. CONCLUSIONS

We have analysed three new XMM-Newton observations of the M31 dipping LMXB Bo 158, in addition to re-analysing the three observations discussed in Tru-

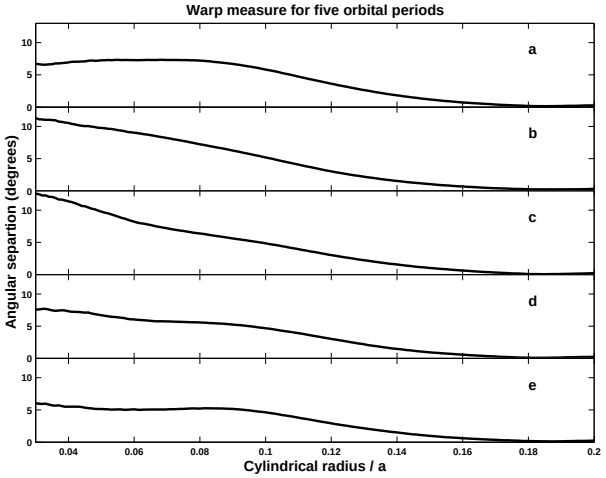

Figure 4. Radial warp profiles. The vertical axis is the warp amplitude. The horizontal axis is distance from the primary object normalized such that the binary separation is 1. *Plots (a), (b), (c), (d) and (e) are for five consecutive orbital cycles.*

dolyubov et al. (2002). The newer observations spanned $\sim$3 days in 2004, July. We find that that the relationship between source intensity and depth of dipping is not so simple as described by Trudolyubov et al. (2002). Instead, we believe that the observed variation in dipping behaviour is caused by precession in the accretion disc; dipping would be confined to a limited phase range in the disc precession cycle.

We modelled the accretion disc with 3D SPH, and found prograde disc precession on a 81 ± 3 hr period, as well as radiatively driven disc warp that precessed on a 31 hr period in a retrograde fashion. We find that the disc precession is most likely to affect the observed dipping behaviour. Hence, we predict that the dipping behaviour of Bo 158 experiences a 81 ± 3 hour cycle; this period is consistent with the observed variation of the dips.

REFERENCES

Barnard, R., Church, M. J., & Bałucińska-Church, M. 2003, A&A, 405, 237

Battistini, P., Bonoli, F., Braccesi, A., et al. 1987, A&AS, 67, 447

Chou, Y., Grindlay, J. E., & Bloser, P. F. 2001, ApJ, 549, 1135

Church, M. J. & Bałucińska-Church, M. 1995, A&A, 300, 441

Church, M. J. & Bałucińska-Church, M. 2004, MNRAS, 348, 955

Church, M. J., Dotani, T., Balucinska-Church, M., et al. 1997, Apj, 491, 388

Church, M. J., Parmar, A. N., Balucinska-Church, M., et al. 1998, A&A, 338, 556

Di Stefano, R., Kong, A. K. H., Garcia, M. R., et al. 2002, ApJ, 570, 618

Eggleton, P. P. 1983, ApJ, 268, 368

Foulkes, S. B., Haswell, C. A., Murray, J. R., & Rolfe, D. J. 2004, MNRAS, 349, 1179

Foulkes, S. F., Haswell, C. A., & Murray, J. R. 2006, MNRAS, submitted

Frank, J., King, A. R., & Raine, D. 2002, Accretion Power in Astrophysics, 3rd Edition (Cambridge University Press)

in't Zand, J., Verbunt, F., Heise, J., et al. 2004, To appear in "The Restless High-Energy Universe" (2nd BeppoSAX Symposium), eds. E.P.J. van den Heuvel, J.J.M. in 't Zand & R.A.M.J. Wijers, Nucl. Instrum. Meth. B Suppl. Ser, astro-ph/0403120

Larwood, J. D. & Papaloizou, J. C. B. 1997, MNRAS, 285, 288

Murray, J. R. 1996, MNRAS, 279, 402

Murray, J. R. 1998, MNRAS, 297, 323

Nauenberg, M. 1972, Apj, 175, 417

Ogilvie, G. I. & Dubus, G. 2001, MNRAS, 320, 485

Osaki, Y. 1989, PASJ, 41, 1005

Press, W. H., Flannery, B. P., & Teukolsky, S. A. 1986, Numerical recipes. The art of scientific computing (Cambridge: University Press, 1986)

Pringle, J. E. 1996, MNRAS, 281, 357

Retter, A., Chou, Y., Bedding, T. R., & Naylor, T. 2002, MNRAS, 330, L37

Shakura, N. I. & Sunyaev, R. A. 1973, A&A, 24, 337

Smale, A. P., Mason, K. O., White, N. E., & Gottwald, M. 1988, MNRAS, 232, 647

Trudolyubov, S., Borozdin, K. N., Priedhorky, W. C., et al. 2002, ApJL, 581, L27

Truss, M. R., Murray, J. R., Wynn, G. A., & Edgar, R. G. 2000, MNRAS, 319, 467

van den Bergh, S. 2000, The galaxies of the Local Group, Cambridge University Press, Cambridge Astrophysics Series Series, vol no: 35

Vogt, N. 1974, A&A, 36, 369

Warner, B. 1975, MNRAS, 170, 219

White, N. E. & Swank, J. H. 1982, ApJL, 253, L61

Whitehurst, R. & King, A. 1991, MNRAS, 249, 25